

# Modelling and Inversion-based Control of a Magnetorheological Vehicle Suspension

H. Sleiman<sup>1, 2</sup>, B. Lemaire-Semail<sup>3</sup>, S. Clénet<sup>2</sup>, J. Lozada<sup>1</sup>

1: CEA LIST, Sensory Interfaces Laboratory, 18, route du Panorama, BP6, FONTENAY AUX ROSES, F- 92265 France

2: ENSAM, L2EP, F -59000 Lille, France

3: Université Lille Nord de France, L2EP F- 59000 Lille, France

[Betty.semail@polytech-lille.fr](mailto:Betty.semail@polytech-lille.fr),

Type: Regular paper, preferred presentation: oral, technical track 1: Vehicular electric power systems and loads

**Abstract-** *In this paper, we present the development, modelling, and simulation of two semi-active control strategies applied on a magnetorheological (MR) suspension for automotive applications. A modified Sky-Hook strategy and a new control strategy based on the inversion of the Energetic Macroscopic Representation of the MR suspension are considered. A special scaled-down test bench is designed and manufactured to characterize the MR damper. Simulation results of both control strategies are shown and discussed especially from electrical energy consumption point of view as this is one of the key criteria for the design of new vehicles.*

Key words: Magnetorheological damper, semi-active control, Energetic Macroscopic Representation, vehicle suspension.

## 1. Introduction

In the automotive field, suspensions are designed to satisfy several conflicting requirements, such as adequate ride quality, road holding, and handling and control characteristics within the limited clearance space [1]. Active suspensions seem to be the best compromise between comfort and road holding. However, these suspensions are still rare, because of their complexity, cost, energy consumption and the risk of instability inherent in any active system.

To solve these stability problems and to decrease energy consumption, current research also focuses on semi-active suspensions for which various technologies emerged and are already commercialized. Semi-active systems are devices having properties that can be adjusted in real time but they remain passive, thereby they are infinitely stable especially those based on magnetorheological dampers commonly called, MR dampers.

MR fluids are suspensions of micron sized ferromagnetic particles in a carrier liquid (mineral or silicon oil, for example) which apparent viscosity can change under an external magnetic field in milliseconds. Thereby, they are used in a lot of controllable systems [2, 3]. Semi-active suspensions based on MR dampers show a great development, because of their mechanical simplicity, high dynamic range, low power consumption, high force capacity and robustness [4].

In this paper, first we present the problematic of controlling semi-active suspension using the quarter-vehicle model. Sky-Hook and inversion-based control models are explained. Then the experimental test bench used and typical experimental characterization results are shown. Control strategies are implemented into Matlab-Simulink<sup>TM</sup>, and a performance comparison is presented.

## 2. Semi-active control strategies

The control strategies developed for the MR suspension in this study are designed and applied on a quarter-vehicle approach. This model has been widely used to investigate the performance of suspension systems (passive, active and semi-active). Fig. 1 shows a simplified quarter-vehicle model. It consists of a suspended mass of chassis  $m$ , supported by a MR damper in parallel with a spring  $k$ , which in turn is connected to the wheel. The wheel is supposed to be very rigid and consequently, its movement represents the disturbances coming from the road. In other words, we suppose that the road irregularities are directly transmitted to the suspension. This allows us to focus only on the performance of the suspension regarding the input disturbances.

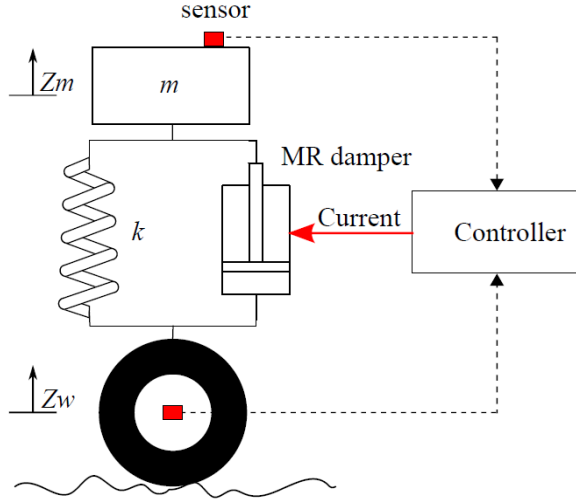


**Figure 1: illustration of the semi-active suspension based on quarter-vehicle model**

Fig. 1 also shows the schematic diagram of the semi-active control. Two sensors are placed respectively on the mass and on the wheel. Information coming from these sensors are sent to the controller which calculates the necessary input current to the MR damper, according to the control strategy. From this figure, the dynamic relationship applied to the chassis gives:

$$m\ddot{z}_m = -F_s - F_d - mg \quad (1)$$

where

$$F_s = k(z_m - z_w) \quad (2)$$

is the spring force and

$$F_d = c(v_m - v_w) + F_{MR} \quad (3)$$

is the total damping force.  $z_m$  and  $v_m$  are respectively the displacement and velocity of the chassis,  $z_w$  and  $v_w$  those of the wheel and  $c$  the viscous damping coefficient. In (3)  $F_{MR}$  is the MR controllable component of the total damping force and it depends on the intensity of the applied current  $i$  in the damper. According to a Bingham rheological behaviour [5] of the MR fluid, this force is given by:

$$F_{MR} = c' i \operatorname{sgn}(v_m - v_w) \quad (4)$$

$c'$  is a coefficient depending on the damper's characteristics and the sign function implies that the force is always opposed to the relative velocity of the damper. It is a resistive force, only the intensity of this force can be controlled. The parameters of these forces are experimentally identified.

### 2.1. Modified Sky-Hook control strategy

The first control law tested in this work is based on the Sky-Hook control which can be described as follows:

$$\text{if } \begin{cases} v_m(v_m - v_w) \geq 0 \Rightarrow \text{damper on} \\ v_m(v_m - v_w) < 0 \Rightarrow \text{damper off} \end{cases} \quad (5)$$

This strategy indicates that if the relative velocity of the body with respect to the wheel is in the same direction as that of the body velocity, then a maximum damping force should be applied to reduce the body acceleration. On the other hand, if the two velocities are in the opposite directions, the damping force should be at a minimum to minimize body acceleration [6]. However in this work, the Sky-Hook strategy is slightly improved: the damper is not activated according to an on-off control, but the calculated input current depends on the absolute body velocity. Typically, electrical current is no longer the maximum current admissible by the MR damper, but it is chosen such that the MR force is proportional to the absolute velocity of the chassis. Assuming that  $b$  is the coefficient of proportionality, the MR force becomes:

$$F_{MR} = b v_m \quad (6)$$

Replacing  $F_{MR}$  by its expression in (4), we obtain for the necessary input current:

$$i = \frac{b v_m \operatorname{sgn}(v_m - v_w)}{c'} \quad (7)$$

However, according to the strategy of Sky-Hook control, the damper is activated only if  $v_m(v_m - v_w) \geq 0$ . Therefore, the expression of the input current is:

$$i = \frac{b |v_m|}{c'} \quad (8)$$

This modified Sky-Hook control allows adapting the electrical power consumption according to the extent of the disturbances and mass movement.

## 2.2. Inversion-based control

### 2.2.1 Energetic Macroscopic Representation (EMR) of the MR suspension

EMR is based on the action-reaction principle to organize the interconnection of the sub-systems according to the physical causality (i.e. integral causality) [7]. This description highlights energetic properties of the system (energy accumulation, conversion and distribution). The EMR of the quarter-vehicle suspension is depicted on the upper part of Fig. 2 (orange pictograms). Each mechanical or electrical element is represented by a specific pictogram corresponding to its function. A summary of equivalent pictograms can be found in the appendix. From left to right, the different parts are described as follows:

a) Mechanical source

b) Parallel connection

c) Spring

$$F_s = \int k(v_m - v_w)dt \quad (10)$$

d) Damper

$$F_{MR} = c(v_m - v_w) + c' i \operatorname{sgn}(v_m - v_w) \quad (11)$$

e) Parallel connection:

$$\begin{cases} \text{common } v_m \\ F_{tot} = F_d + F_s \end{cases} \quad (12)$$
$$m \frac{d}{dt} v_m = -F_{tot} - m.g \quad (13)$$

### 2.2.2 Inversion-based control of the quarter-vehicle suspension

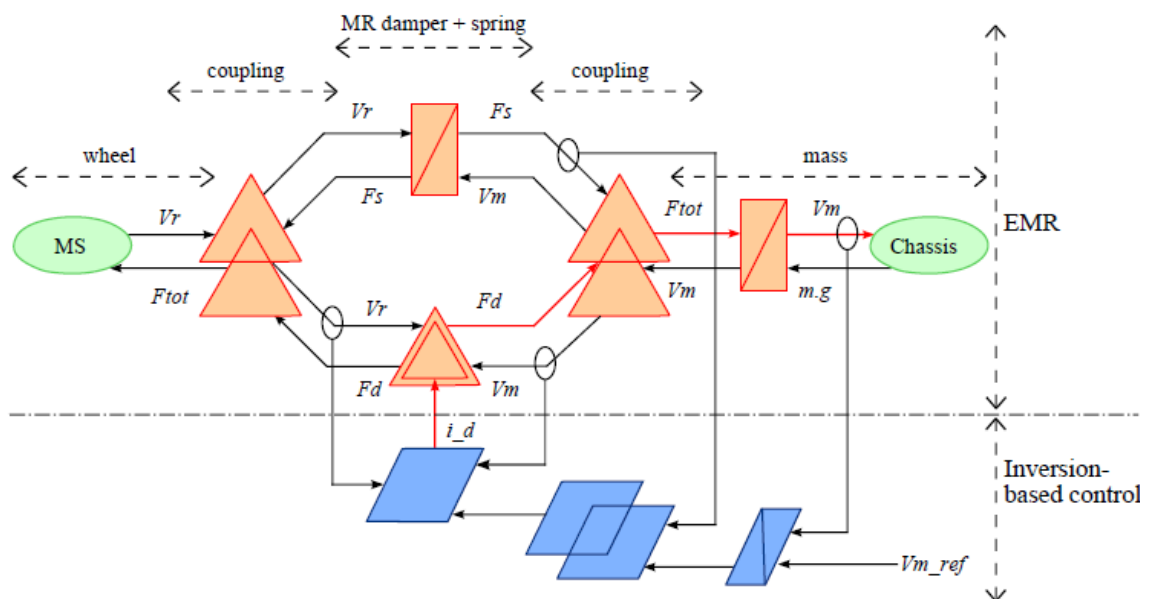


**Figure 2: EMR and control structure of the quarter-vehicle MR suspension**

Thus the control has to express the tuning input  $i$  as a function of the output set point  $V_m$ . On a horizontal road, we could choose for example  $V_{m\_ref}=0$  in order to minimize the vibration of the chassis.

The tuning chain links the tuning input to the global output to be controlled and the control chain is obtained by inverting the tuning chain step by step using inversion rules. According to the objective, the tuning chain (red arrows) chosen is:

$$i \rightarrow F_d \rightarrow F_{tot} \rightarrow V_m$$

then control chain is obtained:

$$i \leftarrow F_{d\_ref} \leftarrow F_{tot\_ref} \leftarrow V_{m\_ref}$$

The lower part of Fig. 2 represents the control structure deduced by the EMR of the quarter vehicle model, from right to left we have:

(a) Inversion of the chassis

This element is an accumulation element. A controller is needed to define the total suspension force  $F_{tot\_ref}$  from the chassis velocity  $V_{m\_ref}$ :

$$F_{tot\_ref} = C(v_{m\_ref} - v_{m\_mea}) \quad (13)$$

Where  $C$  is the controller ( $P$ ,  $PI$  or other types of controller) and  $v_{m\_mea}$  is the experimental value measured by a sensor, for example, by integrating an accelerometer signal placed on the chassis. On fig. 2, sensors are represented by small circles on the arrows corresponding to the required variables.

(b) Inversion of the mechanical coupling

From this block, we can deduce the damping force  $F_{d\_ref}$ :

$$\begin{aligned} F_{tot\_ref} &= F_{d\_ref} + F_s \\ \Rightarrow F_{d\_ref} &= F_{tot\_ref} - F_s \end{aligned} \quad (14)$$

with  $F_s$  is the spring force.

(c) Inversion of the damper

This last inversion of the tuning chain aims at finding the necessary input current in the damper:

$$\begin{aligned} F_{d\_ref} &= c(v_{m\_mea} - v_{w\_mea}) \\ &\quad + c' i \operatorname{sgn}(v_{c\_mea} - v_{w\_mea}) \\ \Rightarrow i &= \frac{F_{d\_ref} - c(v_{m\_mea} - v_{w\_mea})}{c' \operatorname{sgn}(v_{c\_mea} - v_{w\_mea})} \end{aligned} \quad (15)$$

$v_{w\_mea}$  is measured by a sensor placed on the wheel axle.

Note that informations coming from the two sensors are also used to evaluate the spring force  $F_s$ .

### 3. Characterization set up

Fig. 3 shows a picture of the experimental set-up developed to identify the parameters of the scaled-down MR damper. This damper was conceived with a scale factor between the forces of the scaled-down damper and a real vehicle damper of about 1/50.

The damper is actuated by a linear motor which simulates the wheel vibrations. The damping force is measured using a force sensor placed above the damper. A LVDT linear position sensor is placed at the piston rod level, the velocity is obtained by the derivation of position signal. Testing of the damper involves axial extensions and compressions with profile motion at different velocities while simultaneously subjecting the damper to varying currents. Measuring of electrical properties of the damper coil gives for the resistance  $R=1.7\Omega$  and for the inductance  $L=5\text{mH}$ . Fig. 4 presents force/velocity graph for values of electrical current from 0A to 1.5A, and fig. 5 shows the corresponding force/current graph. As mentioned above, the dynamic behaviour of the damper is assimilated to a Bingham model written as follows:

$$F_{MR} = cv + c' i \operatorname{sgn}(v) \quad (16)$$

where  $v$  is the relative displacement of the damper piston and  $i$  the input current.

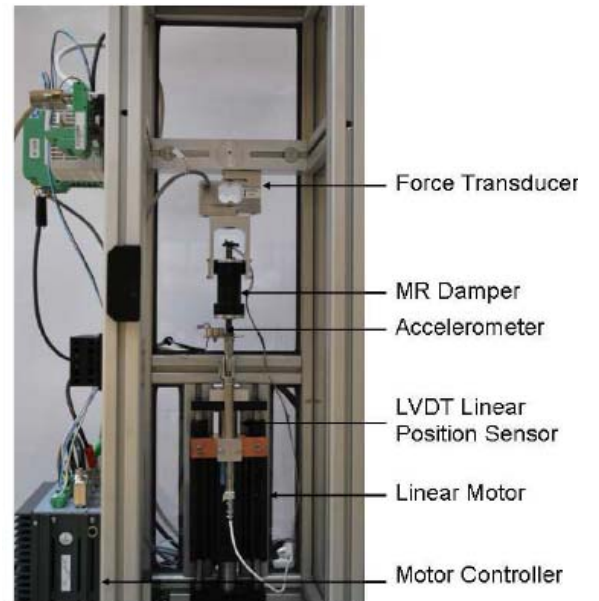


Figure 3: Dynamic experimental test bench of the MR damper

By identification and taking into account only the linear part of the force vs. velocity and force vs. current evolution, we find  $c=55 \text{ N.s.m}^{-1}$  and  $c'=49 \text{ N.A}^{-1}$ .

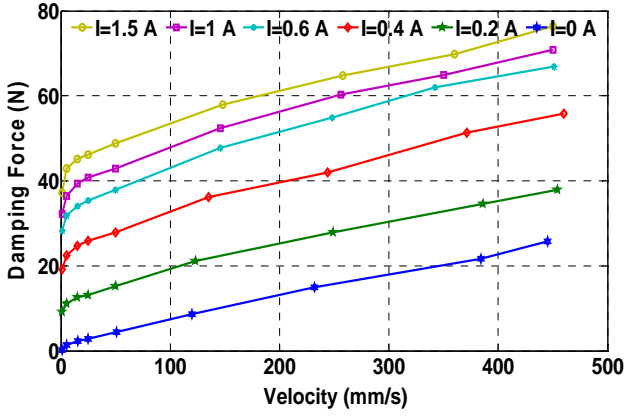


Figure 4: Damping force vs. velocity for different current values.

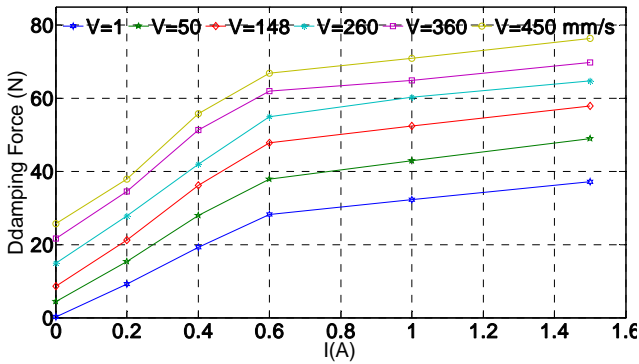


Figure 5: Damping force vs. current for different velocity levels.

#### 4. Simulations and Control performances

EMR and inversion-based control can be directly transposed to Matlab-Simulink™ scheme (Fig. 6). In the simulation model, a stiffness spring of  $6200 \text{ N.m}^{-1}$  and a mass of  $3.6 \text{ kg}$  were chosen. Thus, the resonant frequency of the system is  $\sqrt{k/m}/2\pi = 6.6 \text{ Hz}$ .

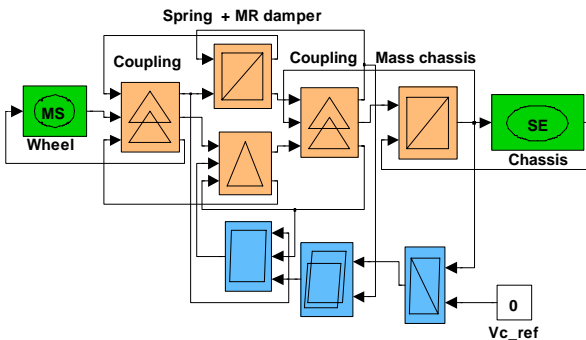


Figure 6: Matlab-Simulink™ model of the MR quarter-vehicle MR suspension.

The controller chosen is a proportional controller. The choice of its gain  $P$  is determined by identifying the closed loop transfer function to a second order system with a damping rate  $\xi = 0.7$ . To assess the effectiveness of each control law (Sky-Hook control

and inversion-based control), we apply a sinusoidal excitation to the quarter-vehicle model. The movement frequency is  $6.6 \text{ Hz}$  which corresponds to the resonance frequency; vibrations are thus amplified and therefore we can better visualize the effect of each control law.

#### 4.1 Simulation results

Fig. 7 shows the position of the chassis and the influence of each control law. The results are quite close: Sky-Hook control reduces the amplitude of vibration by  $67\%$  while the inversion-based control reduces vibration by  $63\%$ , this gives a benefit of  $4\%$  in terms of comfort for the first one but it may not be significant. However, the efficiency of the both control laws is noteworthy, in comparison with the case (unrealistic) without any control. On the other hand, according to the Fig. 8, the power consumption during one period for the Sky-Hook strategy is  $0.25 \text{ W}$  and for those based on the inversion of the EMR,  $0.18 \text{ W}$ , making a reduction of  $25\%$  of the electrical power consumption.

#### 5. Conclusion

In this paper two control strategies for vehicle MR suspension are presented. The Shy-Hook control strategy and a new control strategy based on the inversion of the EMR of the quarter-vehicle suspension is introduced. The EMR is associated to macroscopic modelling of the overall system. A reduced scale experimental set-up is presented, which allows parameter identification of the MR damper. Then, simulation results are compared for the two control strategies. the inversion-based control deduced from the EMR of the quarter-vehicle MR suspension yields good performances of the vibration reduction especially from energy consumption point of view.

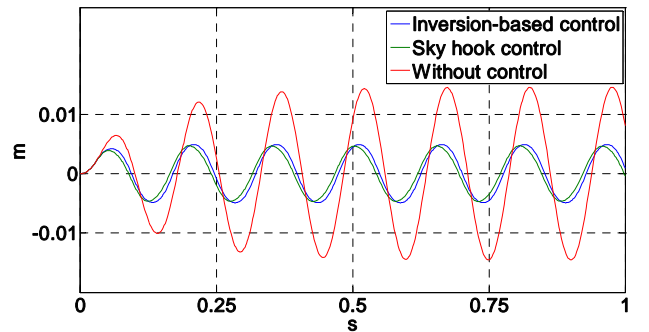
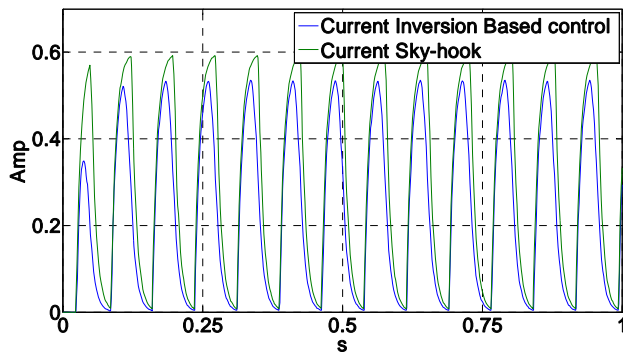


Figure 7: Chassis position for different control strategies.





**Figure 8: Current consumption for the Sky-Hook and inversion based control strategies.**

## Bibliography

- [1] En Rang Wang, Xiao Qing Ma, S. Rakheja et C. Y. Su. Semi-active Control of Vehicle Vibration with MR-dampers. In Conference on Decision and Control, volume 3, pages 2270–2275, 2003.
- [2] G.Yang. “Large-scale magnetorheological fluid damper for vibration mitigation: modelling, testing and control.” Ph.D thesis, University of Notre Dame, Indian, (2001)
- [3] S. Guo, S. Yang, and C. Pan. “Dynamic Modeling of Magnetorheological Damper Behaviors”. Journal of Intelligent Material Systems and Structures 2006; 17; 3.
- [4] M.R. Jolly, J.W. Bender et J.D. Carlson. Properties and applications of commercial magnetorheological fluids. Journal of Intelligent Material Systems and Structures, vol. 10, n° 1, pages 5–13, 2000.
- [5] Stanway, R., Sproston, J.L. and Stevens, N.G. 1987. “Non-linear Modeling of an Electrorheological Vibration Damper,” J. Electrostatics, 20(2):167–184.
- [6] Y. Wu et B. Xu. Study on the damping fuzzy control of semi-active suspension. In Vehicle Electronics Conference, 1999.(IVEC’99) Proceedings of the IEEE International, pages 66–69, 1999.
- [7] PJ Barre, A. Bouscayrol, P. Delarue, E. Dumetz, F. Giraud, JP Hautier, X. Kestelyn, B. Lemaire-Semail et E. Semail. *Inversion-based control of electromechanical systems using causal graphical descriptions*. In Proc. of IEEE-IECON, volume 6, pages 5276–5281, 2006.
- [8] K. Chen, Y. Cheng, A. Bouscayrol, C. Chan, Berthon, Shumei Cui, "Inversion-based control of a

Hybrid Electric Vehicle using a Split Electric Variable Transmission", VPPC’08, Harbin, China, 9-2008

## Appendix: Pictograms of EMR elements and their corresponding inversions [8]

	Source of energy
	Electrical converter (without energy accumulation)
	Mechanical converter (without energy accumulation)
	Electromechanical converter (without energy accumulation)
	Element with energy accumulation
	Element with energy accumulation
	Control block with controller